

# Quantum metrology in Lipkin-Meshkov-Glick critical systems

Giulio Salvatori and Antonio Mandarino

*Dipartimento di Fisica, Università degli Studi di Milano, I-20133 Milan, Italy*

Matteo G.A. Paris\*

*Dipartimento di Fisica, Università degli Studi di Milano, I-20133 Milan, Italy and  
CNISM, Udr Milano, I-20133 Milan, Italy*

The Lipkin-Meshkov-Glick (LMG) model describes critical systems with interaction beyond the first-neighbor approximation. Here we address quantum metrology in LMG systems and show how criticality may be exploited to improve precision. At first we focus on the characterization of LMG systems themselves, i.e. the estimation of anisotropy, and address the problem by considering the quantum Cramér-Rao bound. We evaluate the Quantum Fisher Information of small-size LMG chains made of  $N = 2, 3$  and 4 lattice sites and also analyze the same quantity in the thermodynamical limit. Our results show that criticality is indeed a resource and that the ultimate bounds to precision may be achieved by tuning the external field and measuring the total magnetization of the system. We then address the use of LMG systems as quantum thermometers and show that: i) precision is governed by the gap between the lowest energy levels of the systems, ii) field-dependent level crossing is a metrological resource to extend the operating range of the quantum thermometer.

PACS numbers: 75.10.Jm, 64.60.an, 03.65.Ta

## I. INTRODUCTION

During the last decade a plentiful contamination between condensed matter physics and quantum information theory has been exploited. On the one hand, many body systems exhibiting quantum phase transitions (QPTs), usually studied in terms of order parameters, correlation lengths and symmetry breaking [1] have been fruitfully analyzed in terms of quantum information based tools, such as dynamics of correlation in the ground state (GS) of the systems [2] and quantum information geometry [3–7]. On the other hand, quantum critical systems have been shown to provide a resource for quantum estimation and metrology, offering superextensive precision in the characterization of coupling parameters and thermometry [8–10].

The keystone of quantum estimation theory (QET) resides in the quantum version of the Fisher Information [11, 12], a measure that accounts for the statistical distinguishability of a quantum state from its neighboring ones. Indeed, the geometrical approach to QPT has shown how to improve estimation strategies for experimental inaccessible parameter by driving the system towards critical points, where a sudden change in the ground state structure takes place [8, 13]. In particular this behaviour has been tested in models where the interaction is restricted to first neighbors [9, 10, 14], e.g. quantum Ising and X-Y models in an external field, in order to precisely estimate the parameters of the system and to provide useful information about the phase diagram. In view of the attention paid to systems with more sophisticated interaction among lattice sites [15–18] a question thus naturally arises on whether criticality may be exploited to enhance metrology in systems with interaction beyond the first-neighbor approximation.

In this framework, systems described by the Lipkin-

Meshkov-Glick (LMG) model provide non trivial examples to assess quantum criticality as a resource for quantum estimation. LMG was first proposed as a simple test for many-body problems approximations [19–21] and since then it has been used to describe the magnetic properties of several molecules, remarkably  $\text{Mn}_{12}\text{Ac}$  [22]. It also found applications in several different fields, leading to a variety of results in terms of entanglement properties of its ground state [23–25] and spin squeezing [26]. For finite size chains LMG have been characterized in terms of fidelity susceptibility [27–29] and adiabatic dynamics [30–32]. Although the LMG model cannot be solved analytically for a generic chain size, some of its extensions are amenable to an exact solution [33]. We also mention that the LMG model received attention not only theoretically: experimental implementations have been proposed using condensate systems in a double well potential [34] or in cavities [35, 36]. It has been also shown that is possible to map the dynamics of such model on circuit QED [37] and ion traps [38] systems.

For what concerns metrology, the crucial feature of the LMG model is that its Hamiltonian depends on two parameters: one is the anisotropy parameter, not accessible to the experimenter, while the other is the external magnetic field, thus experimentally tunable, at least to some extent, in order to drive the system towards criticality.

In this paper, we address quantum metrology in LMG systems. We first consider the characterization of LMG systems, i.e. the estimation of anisotropy, and show how criticality may be exploited to improve precision. To this aim we evaluate exactly the quantum Fisher information of small-size LMG chains made of  $N = 2, 3$  and 4 lattice sites and also address the thermodynamical limit by a zero-th order approximation of the system Hamiltonian. Our results show that the maxima of the quantum Fisher information are obtained on the critical lines in the parameter space, i.e. where the ground state of the system is degenerate. We also show that the ultimate bounds to precision may be achieved in practice by tuning

\*Electronic address: matteo.paris@fisica.unimi.it

the external field and by measuring the total magnetization of the system. We also address the use of LMG systems as quantum thermometers, i.e. we consider a LMG chain in thermal equilibrium with its environment and analyze the estimation of temperature by quantum-limited measurements on the sole LMG system. We show that the precision is governed by the gap between the lowest energy levels of the systems, such that the field-dependent level crossing provides a metrological resource to extend the operating range of the quantum thermometer.

The paper is structured as follows: in Section II we briefly review the relevant features of the LMG model in its most relevant forms, whereas in Section III we introduce the tools of quantum estimation theory and establish notation. In Section IV we analyze in details estimation of anisotropy, whereas Section V is devoted to LMG systems as quantum thermometers. A perturbation analysis in order to discuss the robustness of the optimal estimators against fluctuations of the external field is the subject of Section VI. Finally, in section VII we address the thermodynamical limit by means of a zero-th order approximation of the system Hamiltonian. Sec. VIII closes the paper with some concluding remarks.

## II. THE LMG MODEL

In this section we review the main features of the Lipkin-Meshkov-Glick model. As a matter of fact, the model has been widely studied in many branches of science and it is known in several equivalent forms. We present the most relevant ones, with emphasis on the symmetries of the system.

The original formulation [19–21] describes a system of  $N$  fermions occupying two  $N$ -fold degenerated levels separated by an energy gap  $\epsilon$ . Let  $s = -1, 1$  be and index for the level and  $p = 1, \dots, N$  an index exploring the degeneracy of the levels, let us consider a fermion algebra  $\{\alpha_{ps}, \alpha_{p's'}^\dagger\} = \delta_{pp'}\delta_{ss'}$  with  $\alpha_{ps}$  ( $\alpha_{ps}^\dagger$ ) the annihilation (creation) operator of a fermion in the  $p$ -th degenerated state of the  $s$  level, then the LMG Hamiltonian reads

$$H = \frac{\epsilon}{2} \sum_{ps} s \alpha_{ps}^\dagger \alpha_{ps} + \frac{\mu}{2} \sum_{pp's} \alpha_{ps}^\dagger \alpha_{p's}^\dagger \alpha_{p'-s} \alpha_{p-s} + \frac{\nu}{2} \sum_{pp's} \alpha_{ps}^\dagger \alpha_{p'-s}^\dagger \alpha_{p's} \alpha_{p-s}. \quad (1)$$

The first term takes into account the single-particle energies, the second term introduces a scattering between couples of particles in the same level and the third term is a level swapping for a couple of particles with different  $s$ . The model has the advantage of being simple enough to be solved exactly for small  $N$  or numerically for large  $N$ . In fact, the symmetries of the system allows one to reduce the size of the largest matrix to be diagonalized. At the same time, the system is far to be trivial, and allows one to test the goodness of many approximations techniques [39, 40], as well to compare classical and quantum phase transitions [41].

The Hamiltonian in Eq.(1) may be rewritten in terms of

angular momentum operators defined by

$$S_z = \frac{1}{2} \sum_{ps} s \alpha_{ps}^\dagger \alpha_{ps} \quad (2)$$

$$S_+ = \sum_p \alpha_{p+1}^\dagger \alpha_{p-1} \quad S_- = S_+^\dagger$$

and introducing new parameters

$$\nu = -\frac{1}{N}(1+\gamma) \quad \mu = \frac{1}{N}(1-\gamma) \quad \epsilon = -2h, \quad (3)$$

leading to [46] (apart from an energy shift)

$$H = -\frac{1}{N}(1+\gamma)(S^2 - S_z^2 - \frac{N}{2}) - \frac{1}{2N}(1-\gamma)(S_+^2 + S_-^2) - 2h S_z. \quad (4)$$

Finally, upon writing the  $S$  operators as collective spin operators

$$S_\alpha \equiv \frac{1}{2} \sum_{k=1}^N \sigma_\alpha^k,$$

we may rewrite the LMG Hamiltonian as the Hamiltonian acting on the space of  $N$  interacting spin  $\frac{1}{2}$  systems, also exposed to an external field, i.e.

$$H = -\frac{1}{N} \sum_{j < k} (\sigma_x^j \sigma_x^k + \gamma \sigma_y^j \sigma_y^k) - h \sum_k \sigma_z^k \quad (5)$$

where  $\sigma_\alpha^k$  is the Pauli matrix associated to the direction  $\alpha = x, y, z$  of the  $k$ -th spin. The sum is extended over all the spins, thus describing a system where the interaction is not limited to first neighbours. The first term in Eq.(5) introduces a spin-spin interaction whose strength is made anisotropic in the  $xy$  plane by the  $\gamma$  parameter, which is the ratio between the coupling energies in this directions ( $\gamma = 1$  means no anisotropy). Finally the strength of the interaction with the external field is described by the parameter  $h$ .

It is worth to point out some symmetries of the system. At first we notice that the swap  $h \rightarrow -h$  modifies the Hamiltonian as the (unitary) operations of describing *spin flip*, i.e.  $U = \bigotimes_{k=1}^N \sigma_x^k$

$$H(\gamma, h) = U^\dagger H(\gamma, -h) U \quad (6)$$

so that there is no need to study the  $h < 0$  semi-plane, since the eigenvalues here are the same as in the  $h > 0$  case, and the eigenvectors are related by the transformation matrix  $U$ . Similarly, the  $\gamma$  parameter may be taken in the range  $[-1, 1]$  since any map sending this range into  $(-\infty, -1] \cup [1, \infty]$  modifies the Hamiltonian as a  $\pi/2$  rotation around the  $z$  axis, i.e. as the unitary  $V = \bigotimes_{k=1}^N \sigma_z^k$  together with a rescaling of the field

$$H(\frac{1}{\gamma}, h) = V^\dagger H(\gamma, h\gamma) V. \quad (7)$$

The parameter space is therefore restricted to  $(\gamma, h) \in [-1, 1] \times [0, \infty)$ .

The LMG model spectrum has been extensively studied in the thermodynamic limit [23–25, 42–45]. Following the method suggested in [23] the spectrum of  $H$  in the large  $N$  limit is computed using first a Holstein-Primakoff bosonization

$$\begin{aligned} S_+ &= N^{1/2}(1 - a^\dagger a/N)^{1/2}a & S_- &= S_+^\dagger \\ S_z &= N/2 - a^\dagger a, \end{aligned} \quad (8)$$

and considering at most term in  $(1/N)^0$  in the expansion of the square root. Subsequently in order to diagonalize  $H$  a Bogoliubov transformation is performed

$$a = \cosh \Theta b + \sinh \Theta b^\dagger \quad (9)$$

where  $\Theta \equiv \Theta(\gamma, h)$  is chosen such that the Hamiltonian reads (neglecting a constant energy shift)

$$H \stackrel{N \gg 1}{\cong} \Delta(\gamma, h) b^\dagger b. \quad (10)$$

The study of the ground state reveals two phases in the parameter space: for  $h \geq 1$  the system shows an ordered phase with

$$\Delta(\gamma, h) = 2[(h-1)(h-\gamma)]^{1/2}$$

while for  $0 \leq h < 1$  we have a disordered (broken) phase with an energy spacing among levels given by

$$\Delta(\gamma, h) = 2[(1-h^2)(1-\gamma)]^{1/2}.$$

### III. QUANTUM ESTIMATION THEORY

In this section we briefly review the basics of quantum estimation theory and the tools it provides to evaluate bounds to precision of any estimation process involving quantum systems. Let us consider a situation in which the quantum state of a system is known unless for a parameter  $\lambda$ , e.g. a system with a known Hamiltonian in thermal equilibrium with a reservoir at unknown temperature  $T$ . This situation is described by a map  $\lambda \rightarrow \rho_\lambda$  associating to each parameter value a quantum state. In this framework when one measures an observable  $X$  the outcomes  $x$  occur with a conditional probability distribution  $p_X(x|\lambda)$  given by

$$p_X(x|\lambda) = \text{Tr}[P_x \rho_\lambda], \quad (11)$$

where  $P_x$  is the projector onto the eigenspace relative to  $x$ . In order to estimate the value of  $\lambda$  from the data one needs an *estimator*, i.e. a function  $\hat{\lambda} \equiv \hat{\lambda}(x_1, x_2, \dots)$  of the measurement outcomes to the parameter space. Of course one requires some properties for this estimator, primarily to be unbiased

$$E[\hat{\lambda} - \lambda] = \prod_i \sum_{x_i} \hat{\lambda}(x_1, \dots, x_n) - \lambda = 0 \quad \forall \lambda, \quad (12)$$

where  $E[\cdot]$  denotes the mean with respect to the  $n$  identically distributed random variables  $x_i$  and  $\lambda$  the true value of the parameter. Additionally one requires a small variance for the estimator

$$\text{Var}(\lambda, \hat{\lambda}) = E[\hat{\lambda}^2] - E[\lambda]^2, \quad (13)$$

since this quantity measures the overall precision of the inference process. A lower bound for the variance of any estimator is given by the Cramer-Rao theorem

$$\text{Var}(\lambda, \hat{\lambda}) \geq \frac{1}{MF_\lambda}, \quad (14)$$

where  $M$  is the number of independent measurements and  $F_\lambda$  is the Fisher Information (FI) given by

$$F_\lambda = \sum_x \frac{[\partial_\lambda p_X(x|\lambda)]^2}{p_X(x|\lambda)}. \quad (15)$$

An estimator achieving the Cramer-Rao bound is said to be efficient. Although an efficient estimator may not exist for a given data set, in the limit of large samples, i.e. for  $M \gg 1$ , an asymptotically efficient estimator always exist, e.g. maximum likelihood estimator. In summary, once a map  $\lambda \rightarrow \rho_\lambda$  is given it is possible to infer the value of a parameter of a system by measuring an observable  $X$  and performing statistical analysis on the measurements results. Upon choosing a suitable estimator we may achieve the optimal inference, i.e. saturate at least asymptotically the Cramer-Rao bound.

It is clear that different observables lead to a different probability distribution, giving rise to different FIs and hence to different precisions for the estimation of  $\lambda$  [12]. The ultimate bound to precision is obtained upon maximizing the FI over the set of observables. This maximum is the so-called quantum Fisher information (QFI). In order to obtain an expression for the QFI one introduces the symmetric logarithmic derivative (SLD), which is the operator  $L_\lambda$  solving

$$\frac{L_\lambda \rho_\lambda + \rho_\lambda L_\lambda}{2} = \frac{\partial \rho_\lambda}{\partial \lambda}. \quad (16)$$

SLD allow us to rewrite the derivative of  $\rho_\lambda$  so that Eq.( 15) becomes

$$F_\lambda = \sum_x \frac{\text{Re}(\text{Tr}[\rho_\lambda P_x L_\lambda])^2}{\text{Tr}[\rho_\lambda P_x L_\lambda]}, \quad (17)$$

which is upper bounded by

$$F_\lambda \leq \text{Tr}[\rho_\lambda L_\lambda^2] \equiv G_\lambda. \quad (18)$$

where  $G_\lambda$  is the quantum Fisher information. In order to obtain an explicit form for the QFI one has to solve Eq.(16), arriving at

$$L_\lambda = 2 \int_0^\infty dt e^{-\rho_\lambda t} \partial_\lambda \rho_\lambda e^{-\rho_\lambda t}. \quad (19)$$

Then, upon writing  $\rho_\lambda = \sum_n w_n(\lambda) |\psi_n(\lambda)\rangle \langle \psi_n(\lambda)|$  in its eigenbasis, we have

$$L_\lambda = 2 \sum_{nm} \frac{\langle \psi_n | \partial_\lambda \rho_\lambda | \psi_m \rangle}{w_n + w_m} |\psi_n\rangle \langle \psi_m|, \quad (20)$$

and finally

$$G_\lambda = 2 \sum_{nm} \frac{|\langle \psi_n | \partial_\lambda \rho_\lambda | \psi_m \rangle|^2}{w_n + w_m}, \quad (21)$$

with the sum carried over those indexes for which  $w_n + w_m \neq 0$ . Upon rewriting  $\partial_\lambda \rho_\lambda$  in terms of the eigenvectors and the eigenvalues of  $\rho_\lambda$ , we have

$$\partial_\lambda \rho_\lambda = \sum_n \partial_\lambda w_n |\psi_n\rangle \langle \psi_n| + w_n |\partial_\lambda \psi_n\rangle \langle \psi_n| + w_n |\psi_n\rangle \langle \partial_\lambda \psi_n|, \quad (22)$$

and the QFI assumes the following form

$$G_\lambda = \sum_n \frac{(\partial_\lambda w_n)^2}{w_n} + 2 \sum_{n \neq m} \sigma_{nm} |\langle \psi_n | \partial_\lambda \psi_m \rangle|^2, \quad (23)$$

with

$$\sigma_{nm} = \frac{(w_n - w_m)^2}{w_n + w_m}. \quad (24)$$

The first contribution in the Eq. (23) depend solely on the eigenvalues of  $\rho_\lambda$ , i.e. on the fact that  $\rho_\lambda$  is a mixture, whereas the second term depends on the eigenvectors, i.e. it contains the truly quantum contribution to QFI. The two terms are usually referred to as the *classical* and the *quantum* contribution to the QFI, respectively. For pure states the quantum term is the only one contributing to the QFI.

#### IV. ESTIMATION OF ANISOTROPY

The interaction described by the LMG model depends on two relevant parameters: the anisotropy  $\gamma$  and the external field  $h$ . To these it adds the temperature, or equivalently its inverse  $\beta$ , if we allows the system to interact with the environment by exchanging energy. Among these parameters, the external field may be tuned by the experimenter and represents a tool that allows ones to exploit the systems criticality as a resource to reliably estimate the remaining less controllable parameters.

The anisotropy is a typical quantum parameter, that is its variations modify both the eigenvalues and the eigenvectors of the system. Anisotropy is not tunable by the experimenter, since it is part of the intrinsic coupling among spins and represents a specific characteristic of the system. Anisotropy however *does not* correspond to a proper observable. Its characterization may be addressed within the framework of QET and the ultimate bound to the precision of its estimation is set by the corresponding QFI.

We consider here LMG chains in thermal equilibrium with their environment. The map that we mentioned in the previous Section, from parameters space to quantum states is thus given by the canonical Gibbs density matrix

$$\begin{aligned} \rho(\gamma, h, \beta) &= \frac{e^{-\beta H(\gamma, h)}}{Z(\gamma, h, \beta)} \\ &= \sum_n \frac{e^{-\beta E_n(\gamma, h)}}{Z(\gamma, h, \beta)} |n\rangle \langle n|, \end{aligned} \quad (25)$$

where  $Z(\gamma, h, \beta) = \text{Tr}[e^{-\beta H}]$  is the partition function,  $E_n(\gamma, h)$  the  $n$ -th eigenvalue of the Hamiltonian, and  $|n\rangle$  a basis where  $H$  is diagonal, such that  $\rho(\gamma, h, \beta)$  has eigenvalues equal to the Boltzmann weights

$$B_n \equiv B_n(\gamma, h, \beta) = \frac{e^{-\beta E_n(\gamma, h)}}{Z(\gamma, h, \beta)} \quad (26)$$

In order to evaluate the QFI for  $\gamma$ , an in turn the bounds to precision in its estimation, we have to find the eigenvalues and eigenvector as a function of  $\gamma$  and  $h$  and insert them in Eq. (23). To gain some insight into the role of the chain size while maintaining the approach analytic, we have analyzed in details the cases  $N = 2, 3, 4$ . We will address the complementary limit  $N \rightarrow \infty$  in Sec.VII.

Before proceeding with the results we take a preliminary observation: by studying parameter estimation through information geometric tools such as the QFI and the FI one learns that the parameter of interest is easy to estimate in those points where the parametrized quantum state is easily distinguishable (in a statistical sense) from the neighboring ones, corresponding to slightly different values of the parameter. In our case, upon looking at the very form (25) of the quantum state, one sees that for small values of  $\beta$   $\rho$  is almost independent by  $\gamma$ , going toward a uniform mixture of all the eigenstates. In this regime, one thus expects the estimation of  $\gamma$  to be inherently inefficient. On the other hand, high precision is expected in the large  $\beta$  limit, since the mixture is peaked at the ground state, which is intuitively more sensitive on  $\gamma$  fluctuations.

Using Eq.(23) and the results of diagonalization (see Appendix A), one arrives at the QFI  $G_\gamma \equiv G_\gamma(\gamma, h, \beta)$ . For  $N = 2$  the explicit expression is given by

$$G_\gamma = \frac{1}{r^2} \left[ \beta^2 \frac{\kappa_1}{2\kappa_2} + \frac{16h^2}{r^2} \frac{(1 - e^{\beta r})^2}{(1 + e^{\beta r})\sqrt{\kappa_2}} \right], \quad (27)$$

where

$$\begin{aligned} \kappa_1 &= e^{-\frac{1}{2}\beta(v-r)} \left[ \frac{1}{2}(u-r)^2 + 4(8h^2 + u^2)e^{\frac{1}{2}\beta(v+r)} \right. \\ &\quad \left. + \frac{1}{2}(u-r)^2 e^{\beta(v+r)} + \frac{1}{2}(u+r)^2 e^{\beta r} + \frac{1}{2}(u+r)^2 e^{v\beta} \right] \\ \kappa_2 &= \left[ 1 + e^{\beta r} + e^{\frac{1}{2}\beta(v+r)} + e^{-\frac{1}{2}\beta(v-r)} \right]^2 \end{aligned}$$

with  $u = \gamma - 1$ ,  $v = \gamma + 1$  and  $r = \sqrt{u^2 + 16h^2}$ . For  $N = 3$  and  $N = 4$  the expressions are quite cumbersome and we are not reporting them.

Optimal estimation of the anisotropy at fixed temperature may be achieved by maximizing the QFI over the external field  $h$ . Results of this maximization show that the optimal values of the field correspond to the *critical lines* of the model, i.e. the lines in the parameter space corresponding to a degenerated ground state (GS), i.e.

$$N = 2 \rightarrow h_c = \frac{\sqrt{\gamma}}{2} \quad (28)$$

$$N = 3 \rightarrow h_c = \frac{2\sqrt{\gamma}}{3} \quad (29)$$

$$N = 4 \rightarrow h_c = \frac{\sqrt{\gamma}}{4} \text{ and } h_c = \frac{3\sqrt{\gamma}}{4}. \quad (30)$$

For  $N = 2$  the maximized QFI  $G_\gamma(\gamma, \frac{1}{2}\sqrt{\gamma}, \beta)$  is given by

$$G_\gamma^{\text{opt}} = \frac{8\gamma + \kappa^2 + \gamma(\gamma\kappa^2 - 8) \text{sech}^2 \frac{1}{2}\kappa}{4(1 + \gamma)^4} \quad (31)$$

where  $\kappa = \beta(1 + \gamma)$ . In the low temperature regime, i.e.  $\beta \gg 1$  we may write

$$G_\gamma^{\text{opt}} \simeq \beta^2 \frac{(u + r)^2}{8r^2} \begin{cases} e^{\frac{1}{2}\beta(v-r)} & h \geq \sqrt{\gamma}/2 \\ e^{-\frac{1}{2}\beta(v-r)} & h < \sqrt{\gamma}/2 \end{cases} \quad (32)$$

Notice that the exponent is the energy gap between the two lowest energy eigenvalues, which vanishes on the degeneracy line. For  $N = 4$  the absolute maximum corresponds to  $h_c = \frac{3\sqrt{\gamma}}{4}$ . For  $N = 3$  also the condition  $h = 0$  individuates a degenerated GS, but this is not corresponding to a maxima of the QFI for reasons that will be clear in the following.

The role of criticality is illustrated in details in Fig. 1, where we show  $G_\gamma$  as a function of  $\gamma$  and  $h$  for different values of  $\beta$ . As it is apparent from the plots, when the temperature decreases  $G_\gamma$  diverges as  $\beta^2$  on the critical lines, whereas in any other point of the parameter space it assumes a finite value. In other words, for any value  $\gamma \geq 0$  it is possible to tune the external field to an optimal value which drives the system into the degeneracy lines, i.e. into critical points. In this way, one maximizes the QFI and, in turn, optimize the estimation of  $\gamma$ . This results confirm that criticality is in general a resource for estimation procedures. The degeneracy line at  $h = 0$  line for  $N = 3$  is an exception, since no gain in precision is achieved despite a crossing between the two lowest energy states is present. We will address this issue and clarify the point in the following subsection.

#### A. A two-level approximation to assess estimation of anisotropy in the low temperature regime

An intuitive understanding of our findings may be achieved by means of an approximation for the Gibbs states, where we consider only the two lowest levels of the system

$$\rho(\gamma, h, \beta) \propto e^{-\beta E_0} |0\rangle\langle 0| + e^{-\beta E_1} |1\rangle\langle 1| \quad (33)$$

where  $E_{0,1}$  are the smallest eigenvalues. In fact, for the values of  $N$  we have considered, the energy spectra of the Hamiltonians show a common structure: the two lowest eigenvalues, i.e. the GS and the first excited level, cross each other but they remain smaller than the other levels for the whole range of  $\gamma$  and  $h$  values. As a consequence, for large  $\beta$  (i.e. in the low temperature regime) the Boltzmann weights corresponding to the smallest eigenvalues are the only appreciable in the sum in Eq. (25) and the density matrix is well be approximated by the expression in Eq. (33). The approximation is more and more justified as far as  $\beta$  increases. We now proceed by noticing that for the family of states (33), the quantum contribution to  $G(\gamma)$  does not contain any divergent term in  $\gamma$ ,  $h$  or  $\beta$ . This may be easily seen from Eq. (23) and from the fact that the eigenvectors are smooth functions of the parameters. Actually, this is the case also for other first-neighbour models

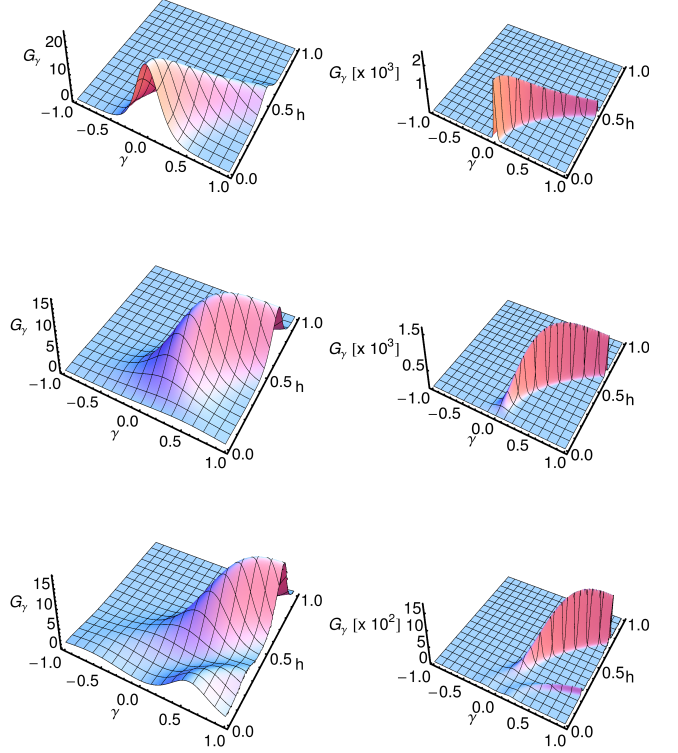


FIG. 1: Estimation of anisotropy in the LMG model. The plots show the QFI  $G_\gamma$  for the anisotropy as a function of the anisotropy parameter  $\gamma$  itself and of the magnetic field  $h$  for two values of  $\beta$ . The panels of the left refer to  $\beta = 10$  while those on the right to  $\beta = 100$ . The rows, from top to bottom, contain the results for  $N = 2, 3, 4$  lattice sites respectively. Comparing the two columns it is clear that  $G_\gamma$  reaches its maximum along the critical lines of the system as  $\beta^2$ , with such divergence modulated also by a non trivial function of  $\gamma$ . Note the peculiar absence of divergence in the  $N=3$  case for  $h=0$ .

[8, 9], so that the approximation here described may apply to other models. We thus introduce a general notation in order to analyze the classical contribution.

Consider a qubit with eigenenergies  $f(a, b)$  and  $g(a, b) = f(a, b) + x(a, b)$ , depending on the parameters  $a$  and  $b$  ( $b$  may also be a set of parameters). With the usual map to the thermal state, the QFI for the parameter  $a$  rewrites

$$G_a(a, b, \beta) = \beta^2 \frac{e^{\beta x(a, b)}}{[1 + e^{\beta x(a, b)}]^2} [\partial_a x(a, b)]^2 \quad (34)$$

It is easy to see that  $G_a(a, b, \beta)$  diverges only in those points  $a_0$  and  $b_0$  such that  $f(a_0, b_0) = g(a_0, b_0)$  and  $\partial_a f(a_0, b_0) \neq \partial_a g(a_0, b_0)$ . When this happens, QFI is proportional to  $\beta^2$ . The two conditions are indeed satisfied on the degeneracy lines mentioned above, except for the case  $N = 3$  and  $h = 0$ , where the partial derivatives of the eigenvalues are equal, thus preventing the divergence of the QFI.

### B. Achieving the ultimate bound to precision using feasible measurements

In the previous Sections we have evaluated the ultimate bound to precision for the estimation of anisotropy, and have shown that the level crossing driven by the magnetic field is a resource for the estimation. In order to exploit this *quantum critical* enhancement one has in principle to implement the measurement of the symmetric logarithmic derivative which, in turn, should be an accessible observable for the LMG system under investigation. Since it is unlikely to have such a control on a quantum system that any observable is measurable, one is generally led to assess estimation procedure based on realistic observables, i.e. to evaluate their Fisher Information and to compare this function with the QFI.

In this section we consider a realistic observable, the total magnetization of the LMG system, and compute the corresponding FI for the estimation of anisotropy. As we will see, this quantity approaches the QFI in the critical region, thus showing that quantum critical enhancement of precision is indeed achievable in an experimentally accessible scenario.

The total magnetization is diagonalized in the basis  $\otimes_{k=1}^N |m_z\rangle_k$ , where  $m_z \in 1, -1$  and  $|x\rangle_k$  denotes the eigenvectors of the  $z$  spin component of the  $k$ -th spin. If  $N_z$  is the number of spins up for a given basis element, the corresponding eigenvalue is simply  $\sum_{k=1}^N i = 2N_z - N$ , and the probability of such measurement outcome, with the notation of Eq.( 15), is given by

$$p(2N_z - N, \lambda) = \frac{\text{Tr}[P_{N_z} \exp -\beta H]}{Z}, \quad (35)$$

where  $P_{N_z}$  denotes the projector onto the subspace spanned by the basis elements with  $N_z$  spins up. Finally, to compute the corresponding Fisher Information  $F_\gamma$  we substitute these probabilities in Eq. (15).

We are not going to report the explicit formula for the  $F_\gamma$ , which is quite unhandy. Rather, we introduce and discuss an approximation which allows us to reproduce its main features. We anticipate that  $F_\gamma$  shares with the QFI the nice behaviour in the critical region, i.e. it diverges as  $\beta^2$  on the degeneracy lines, except for the case  $h = 0$  line for  $N = 3$ .

Let us consider a two-dimensional system prepared in the mixed state  $\rho(\lambda) = p|0\rangle\langle 0| + (1-p)|1\rangle\langle 1|$  where both the eigenvalue  $p$  and the eigenvectors are functions of a parameter  $\lambda$  to be estimated. If a measurement of an observable  $A = x_1|x_1\rangle\langle x_1| + x_2|x_2\rangle\langle x_2|$  is performed, the outcomes are distributed according to

$$P(x_i) = \text{Tr}[\rho|x_i\rangle\langle x_i|] = p|\langle 0|x_i\rangle|^2 + (1-p)|\langle 1|x_i\rangle|^2,$$

where taking into account the normalization of the basis involved, we have the following relations

$$q = |\langle 0|x_1\rangle|^2 = |\langle 1|x_2\rangle|^2 \quad (36)$$

$$1 - q = |\langle 0|x_2\rangle|^2 = |\langle 1|x_1\rangle|^2 \quad (37)$$

We will also denote with  $\delta q = q - (1 - q)$  and  $\delta p = p - (1 - p)$ . With this notation the FI for  $A$  is rewritten in a compact form

as

$$F(\lambda) = \frac{(\partial_\lambda p \delta q + \partial_\lambda q \delta p)^2}{(p \delta q - q)(p \delta q + 1 - q)} \quad (38)$$

Specializing this to the case of our interest we have  $1 - p = \exp(-\beta\epsilon)/Z$  where  $\epsilon = \epsilon(\gamma, h)$  denotes the energy of the first excited level. Without loss of generality we can assume the energy of the GS is to be null, we thus arrive at

$$\partial_\gamma p = \frac{\beta e^{\beta\epsilon}}{[1 + e^{\beta\epsilon}]^2} \partial_\gamma \epsilon. \quad (39)$$

Eq. (39) implies that the FI  $F_\gamma$  of any observable of the form  $A = x_1|x_1\rangle\langle x_1| + x_2|x_2\rangle\langle x_2|$  diverges as  $\beta^2$  in the large  $\beta$  limit, provided that  $\delta q \neq 0$  (this means that the two eigenstates must be distinguishable by that measurement),  $\partial_\gamma \epsilon \neq 0$  (similarly to what we found for the QFI) and that  $\epsilon = 0$ , i.e. that we are at a critical point. Notice that the above model, basically the same we used to explain the results obtained for the QFI, is valid to discuss the estimation performances of the total magnetization, but cannot be used to approximate the FI of *any* observable  $A$  of the LMG model in the limit of low temperature. In fact, even though the state of the system may be always approximated by a qubit, there is no reason for a general observable to be approximated by an operator acting in the qubit space only.

### V. LMG CRITICAL SYSTEMS AS QUANTUM THERMOMETERS

In this section we explore the performances of LMG critical systems as quantum thermometers, i.e. we consider a LMG systems in thermal equilibrium with its environment and analyze the estimation of temperature by quantum-limited measurements on the sole LMG system. In other words, we address the estimation of the temperature, viewed as an unknown parameter of the Gibbs distribution, on the family of states defined in Eq. (25) [47, 48].

Upon inspecting Eq. (25) one easily sees that temperature influences the eigenvalues of the density matrix, but not its eigenvectors, and thus only the classical contribution to the QFI  $G(\beta)$  survives, i.e. the sum depending on the Boltzmann weights in the general expression for QFI of Eqs.( 23). We thus have

$$G_\beta(\gamma, h, \beta) = \sum_{n=1}^d \frac{(\partial_\beta B_n)^2}{B_n}, \quad (40)$$

where  $B_n$  denotes the  $n$ -th Boltzmann weight. It is worth underlining that  $G_\beta(\gamma, h, \beta)$  is equal to the energy fluctuations

mean value over the ensemble, infact

$$\begin{aligned}
 G_\beta(\gamma, h, \beta) &= \sum_{n=1}^d \frac{(\partial_\beta B_n)^2}{B_n} = \\
 &= \sum_{n=1}^d B_n (E_n^2 + (\partial_\beta \ln Z)^2 + E_n \partial_\beta \ln Z) = \\
 &= \overline{E^2} - \overline{E}^2 = \overline{\Delta E^2}
 \end{aligned} \tag{41}$$

In order to assess LMG chains with  $N = 2, 3, 4$  as quantum thermometers we evaluate the QFI and maximize its value by tuning the external field. In Fig. 2 we show the optimal values of field as a function of the anisotropy for different values of  $\beta$  and for sizes of the LMG chain. In contrast to what happened for the estimation of the anisotropy, the optimal values of the field  $h^*$  do not correspond to the critical ones. On the other hand, there is clear connection between the two concepts: for each *critical* line different *optimal* lines exists, correspondingly to slightly larger and slightly smaller values of the field. As the inverse temperature is increased, the optimal lines are smoothly deformed, approaching the corresponding critical one from above and below. This link between critical and optimal lines will be examined in more details later in this section.

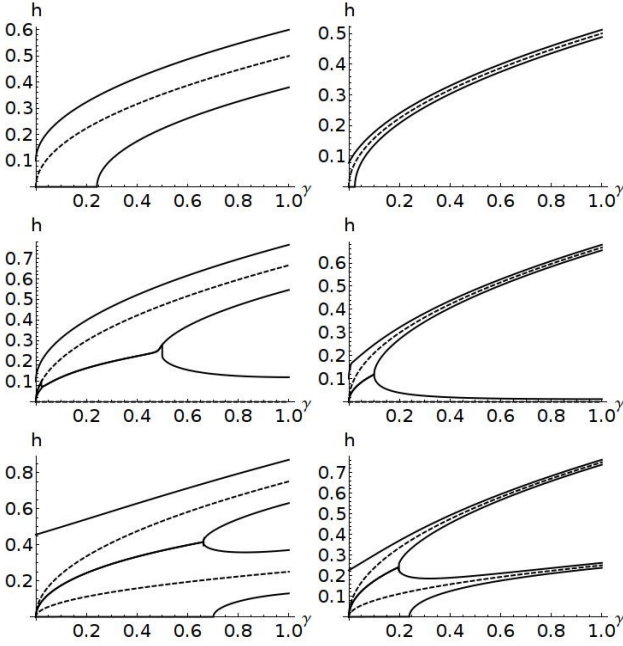


FIG. 2: Quantum thermometry using LMG systems. The plots show the optimal field  $h^*$ , maximizing the QFI  $G_\beta$ , as a function of the anisotropy of the system for different values of  $\beta$  and for different lengths of the LMG chain. Each row show the optimal field versus  $\gamma$  at fixed value of  $N = 2, 3, 4$  respectively. The two columns correspond to  $\beta = 10$  and  $\beta = 100$  respectively. The optimal values of the field are the solid lines whereas the dashed lines are the critical lines  $h_c$  of Eq. (30).

The explicit expression of the QFI  $G_\beta(\gamma, h^*, \beta)$  for  $N = 2$

is given by

$$G_\beta = \frac{1}{2} \frac{\kappa_3}{\kappa_4} \tag{42}$$

where

$$\begin{aligned}
 \kappa_3 &= e^{\frac{1}{2}\beta(v+r)} \left[ \frac{1}{2}(v+r)^2 + 4(1+8h^2+\gamma^2)e^{\frac{1}{2}\beta(v+r)} + \right. \\
 &\quad \left. \frac{1}{2}(v-r)^2 e^{\beta(v+r)} + \frac{1}{2}(v+r)^2 e^{\beta r} + \frac{1}{2}(v+r)^2 e^{\beta v} \right] \\
 \kappa_4 &= \left[ e^{\frac{1}{2}\beta v} + e^{\frac{1}{2}\beta r} + e^{\frac{1}{2}\beta(v+2r)} + e^{\beta(v+\frac{1}{2}r)} \right]^2,
 \end{aligned}$$

with  $v$  and  $r$  as in Eq. (27). Analogue expressions, with several more terms, are obtained for  $N = 3$  and  $N = 4$ : we are not showing the explicit expressions here. In the low temperature regime Eq. (42) may be rewritten as

$$G_\beta \simeq \frac{1}{4}(v-r)^2 \begin{cases} e^{\frac{1}{2}\beta(v-r)} & h \geq \sqrt{\gamma}/2 \\ e^{-\frac{1}{2}\beta(v-r)} & h < \sqrt{\gamma}/2 \end{cases}, \tag{43}$$

where, as in Eq. (32), the exponent is the energy gap between the two lowest energy levels.

In order to gain more insight on the QFI behaviour, in Fig. 3 we show  $G_\beta$  as a function of the anisotropy and of the external field for different values of  $\beta$  and the the number of sites. At first we notice that the presence of optimal lines clearly emerges from the plot. The QFI decreases with  $\beta$  for any value of the anisotropy and the external field and this may easily understood intuitively: as temperature decreases  $\rho(\gamma, h, \beta)$  approaches the projector on the GS space and being this projector independent on the temperature, the QFI vanishes. On the other hand, the quantitative features of the decay, e.g. how fast the optimal  $G_\beta$  tends to zero, are strongly influenced by the criticality of the system. Indeed, outside the critical regions the QFI vanishes exponentially, whereas along the optimal lines it vanishes as  $1/\beta^2$  independently on  $\gamma$ . For increasing  $\beta$  two phenomena occur: i) the optimal lines approach the critical ones,  $h^* \rightarrow h_c$ ; ii) the QFI  $G_\beta$  shows a behavior independent on  $N$ , i.e. Eq. (43) may generalized to  $N = 3, 4$  and rewritten as

$$G_\beta \simeq k(\gamma, h) e^{-\beta f(\gamma, h)} \tag{44}$$

where the functions  $k(\gamma, h)$  and  $f(\gamma, h)$  are non negative, independent on  $\beta$  and zero only on the critical/optimal lines. Overall, we have that the presence of degeneracy, i.e. crossing between the lowest eigenvalues, allow us to find optimal fields where  $G_\beta$  decreases as  $1/\beta^2$ , suggesting that the criticality itself is the reason behind such enhancement.

In order to confirm this intuition and to gain more insight on the QFI behavior in the low temperature regime we again consider the two-level approximation used before. Using the notation of Eq. (34), the QFI rewrites

$$G_\beta(a, b, \beta) = \frac{e^{\beta x(a, b)} [\beta x(a, b)]^2}{[1 + e^{\beta x(a, b)}]^2} \frac{1}{\beta^2} = \frac{F(\beta x(a, b))}{\beta^2}, \tag{45}$$



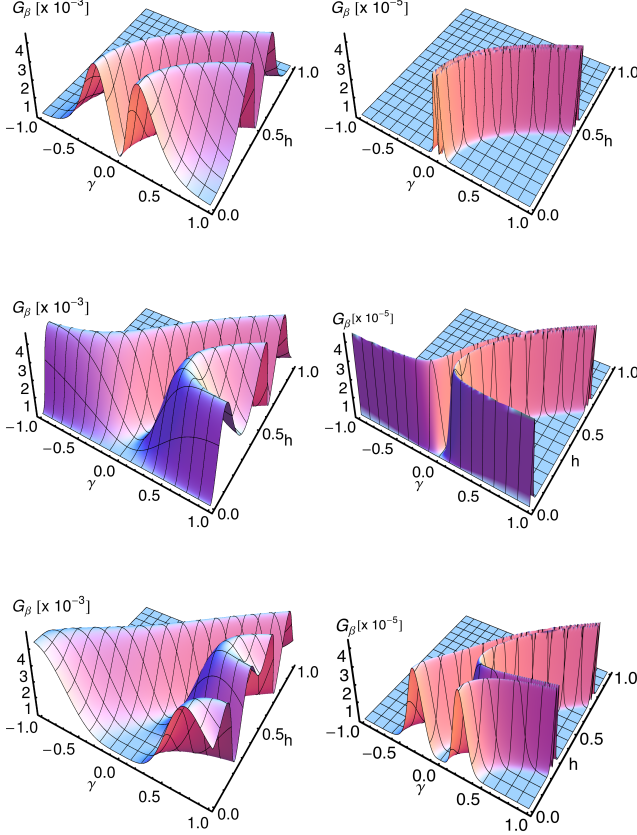


FIG. 3: Quantum thermometry using LMG systems. The plots show  $G_\beta$  versus  $\gamma$  and  $h$  for different  $\beta$  and number of sites. The three rows report results for  $N = 2, 3, 4$  respectively. The two columns refer to  $\beta = 10$  and  $\beta = 100$ .

where  $F(y)$  is a symmetric function vanishing in the origin,  $F(0) = 0$ , and it shows two global maxima at  $y = \pm y_{opt}$ . This explains the behavior shown in Fig. 2 and 3 where for each critical line, i.e.  $x(a, b) = 0$ , two optimal lines are present, corresponding to  $\beta x(a, b) = \pm y_{opt}$ . Moreover, the dependence of  $F(y)$  on the product of  $\beta$  with  $x(a, b)$  clarifies why, as  $\beta$  increases, the optimal lines approach the critical ones. Finally, we see that on the optimal lines the QFI vanishes as  $1/\beta^2$  independently on any parameter, since the maximization of  $F(y)$  factored out the parameter dependence. In other words, the precision is basically governed by the energy gap between the two lowest energy levels. This behavior, in the limit of large  $\beta$ , is independent on the actual model, so that the argument may be equally employed to describe any system with an energy spectrum made of two crossing lowest levels well separated from the other levels.

We finally emphasize that the ultimate bound to precision may be practically achieved, since, as shown by Eq. (41) the SLD turns out to be the total energy of the system, which we assume to be measurable.

## VI. ROBUSTNESS AGAINST FLUCTUATIONS OF THE EXTERNAL FIELD

The results reported in the previous Sections shows that criticality is a resource for quantum metrology in LMG systems. As it has been extensively discussed, in order to achieve the ultimate bounds to precision one should tune the external field to the appropriate value, driving the system towards the critical region. A question thus arises on whether and how an imprecise tuning of the external affects the metrological performances of the system.

This issue basically amounts to a perturbation analysis in order to discuss the robustness of the optimal estimators against fluctuations of the external field. The canonical approach to attack this problem would be that of considering the state of the system as a mixture of different ground states, each one corresponding to a different value of the external field, and then evaluating the quantum Fisher information for this family of states. This is a very challenging procedure to pursue, even numerically, and some approximated approach should be employed instead. In fact, it is possible to provide an estimate of this effect by averaging the QFI over a given distribution for the external field: this is an approximation since the QFI is a nonlinear function of the density operator, but it is not a crude one, owing to the small value of fluctuations that we should consider for this kind of perturbation analysis.

In order to obtain a quantitative estimate we assume that the actual value of the external field is normally distributed around the optimal one  $h_c$ , and evaluate the averaged QFI for the anisotropy

$$\overline{G}_\gamma(\beta) = \int dh G_\gamma(\gamma, h, \beta) g_\Sigma(h) \quad (46)$$

as a function of the width  $\Sigma$  of the Gaussian  $g_\Sigma(h)$ , viewed as a convenient measure of the fluctuations (i.e. of the imprecise tuning) of the external field. In particular, we choose the range of  $\Sigma$  as to describe an imprecise tuning of the external field up to  $\pm 5\%$ . In Fig. 4 we show the ratio between the field-averaged QFI and the optimal one

$$\xi = \frac{\overline{G}_\gamma(\beta)}{G_\gamma(\gamma, h_c, \beta)}, \quad (47)$$

as a function of the of the width  $\Sigma$  of the Gaussian distribution, for different value of  $\gamma$  and for different temperatures. As it is apparent from the plots, the ratio is close to unit, showing the robustness of the optimal estimator. The plots also show that the detrimental effects of an imprecise tuning of  $h$  increase with  $\gamma$  and decrease with temperature. Analogue results may be obtained for  $N = 3$  and  $N = 4$  as well as for the estimation of temperature. Overall, we have that the optimal estimators are robust against possible fluctuations of the external field, thus providing a realistic benchmark for precision measurements on LMG systems.



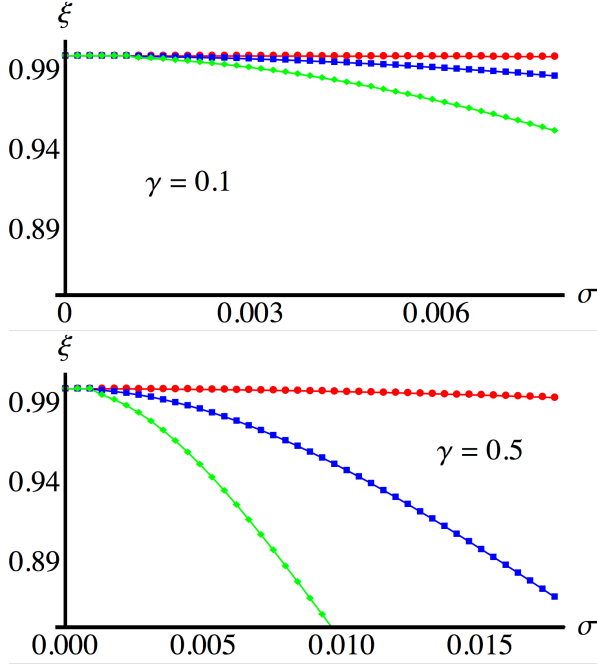


FIG. 4: The ratio  $\xi = \bar{G}_\gamma(\beta)/G_\gamma(\gamma, h_c, \beta)$  between the field-averaged QFI and the optimal one as a function of the width  $\Sigma$  of the field distribution. The upper panel show results for  $\gamma = 0.1$  and the lower one for  $\gamma = 0.5$ . In both panels we show the behavior for  $\beta = 5$  (red points),  $\beta = 25$  (blue squares), and  $\beta = 50$  (green diamonds).

## VII. QUANTUM ESTIMATION IN LARGE LMG SYSTEM: THE THERMODYNAMICAL LIMIT

The study of the thermodynamical limit of the model could be conducted using the diagonal form of the Hamiltonian in Eq.( 10). The family of quantum states we are dealing with may be expressed as  $\rho_\Theta = U_\Theta \rho(\gamma, h, \beta) U_\Theta^\dagger$  where  $U_\Theta = \exp(-i\Theta(\gamma, h)G)$  is a unitary operator,  $G \equiv (a^2 + a^{\dagger 2})$  is the Hermitian operator related to the Bogolyubov transformation in Eq.( 9). This let us to compute the QFIs for anisotropy  $G_\gamma$  and temperature  $G_\beta$  using Eq.( 23), where the parameter  $\lambda$  turns out to be in the first case  $\gamma$  and in the second the inverse temperature  $\beta$ . It is useful to underline that, in the limit of an infinite number of particle the sum in Eq.( 23) is infinite thus leading to region where the quantum Fisher information is divergent.

We do not report here the analytic expressions of the QFIs since they are quite cumbersome. Rather we discuss their behavior analyzing their main features. In Fig. 5 we show  $G_\gamma$  as a function of the external field  $h$  and of the anisotropy  $\gamma$  itself. As it is apparent from the plot, in the ordered phase ( $h > 1$ )  $G_\gamma$  has a finite value everywhere, showing a cusp for  $h$  approaching the critical value. In the broken phase  $G_\gamma$  increases with  $\gamma$  showing a divergent behaviour approaching  $\gamma = 1$  for all value of the magnetic field in the region, thus signaling the sudden change of universality class of the system. In both phases the scaling with the temperature on the critical regions

goes as  $\beta^2$ . More specifically, we have

$$G_\gamma(\gamma, h^*, \beta) \simeq \frac{9}{4(h-1)^2} - \frac{25\beta^2}{12} + O(h), \quad (48)$$

in the orderd phase,  $h > 1$  and

$$G_\gamma(\gamma, h^*, \beta) \simeq \frac{9}{4(\gamma-1)^2} - \frac{25\beta^2(h-1)}{6(\gamma-1)} + O(h), \quad (49)$$

in the broken one, i.e. for  $0 \leq h < 1$ .

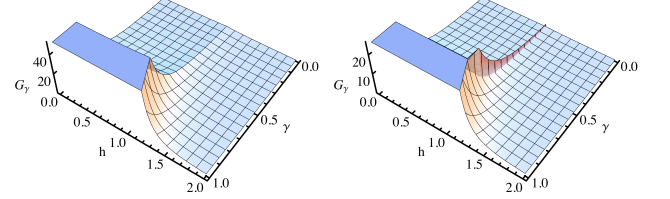


FIG. 5: Characterization of anisotropy in the thermodynamical limit. The plots show the behavior of  $G_\gamma$  for the LMG model as function of the anisotropy parameter  $\gamma$  and the external magnetic field  $h$ . The left panel refers to  $\beta = 1$  and the right one to  $\beta = 10^5$ .

The evaluation of the quantum Fisher information for the temperature shows how it reaches is maximum, without showing divergences, along the degeneracy lines previously outlined, but this time it scales as  $\beta^{-2}$  at the first order near the critical field. If  $h \geq 1$  we have

$$G_\beta(\gamma, h, \beta) \simeq \frac{1}{\beta^2} + \frac{1}{3}(\gamma-1)(h-1) + O(h^{\frac{3}{2}}) \quad (50)$$

instead in the other phase where  $0 \leq h < 1$  we obtain

$$G_\beta(\gamma, h, \beta) \simeq \frac{1}{\beta^2} - \frac{2}{3}(\gamma-1)(h-1) + O(h^{\frac{3}{2}}). \quad (51)$$

We notice that this results could be improved only going beyond the Gaussian approximation performed in Eqs.( 8, 9) since in the broken phase region the effective separation between the degenerate ground state vanishes as  $\exp(-N)$ . As a matter of fact, it would be possible to recover the results obtained for the finite chain cases, i.e. divergences along  $h^* \simeq \sqrt{\gamma}$ , only looking at the fine structure of the level in the broken phase.

## VIII. CONCLUSIONS

We have addressed quantum metrology in LMG model as a paradigmatic example of criticality-assisted estimation in systems with interaction beyond the first-neighbor approximation. In particular, we analyzed in details the use of criticality in improving precision of measurement procedures aimed at estimating the anisotropy of the system or its temperature.

Upon considering LMG systems in thermal equilibrium with the environment we have evaluated exactly the quantum Fisher information of small-size LMG chains made of  $N = 2, 3$  and 4 lattice sites and analyzed the same quantity in the thermodynamical limit by means of a zero-th order approximation of the system Hamiltonian. In this way we proved that quantum criticality of the system represents a resource in estimating the anisotropy. In fact, the quantum Fisher information  $G_\gamma$  is maximized at the critical lines, where, in the low temperature regime, it diverges as  $\beta^2$ , while being finite everywhere else. We have then shown that the ultimate bounds to precision may be achieved by tuning the external field and by measuring the total magnetization of the system.

We have also addressed the use of LMG systems as quantum thermometers showing that: i) precision is governed by the gap between the lowest energy levels of the systems, ii) field-dependent level crossing provides a resource to extend the operating range of the quantum thermometer. Our results are encouraging for the emergent field of quantum thermometry. Indeed, despite the fact that the QFI  $G_\beta$  vanishes everywhere for decreasing temperature, criticality continues to represent resource: the QFI is maximized along optimal lines approaching the critical ones for decreasing temperature, and there the optimal QFI vanishes as  $1/\beta^2$  instead of exponentially.

Finally, we have introduced a simple model, based on a two-level approximation of the system, which allows us to provide an intuitive understanding of our findings for both  $G_\gamma$  and  $G_\beta$ . Our model also suggests that similar behaviors may be expected for a larger class of critical systems with interaction beyond the first-neighbor approximation.

### Acknowledgments

We acknowledge A. Lascialfari and G. Coló for useful discussions. This work has been supported by the MIUR project FIRB-LiCHIS-RBFR10YQ3H.

### Appendix A: LMG systems with $N = 2, 3, 4$ sites

Here we provide the explicit expression, in the computational basis, of the Hamiltonian for LMG systems with  $N = 2, 3, 4$  sites, as well as the eigenvalues and eigenvectors for  $N = 2, 3$ . Throughout the Section we use the shorthand  $u = (\gamma - 1)$  and  $v = (\gamma + 1)$ .

#### 1. N=2

The matrix form of the two-site LMG Hamiltonian in the computational basis reads as follows

$$H_2 = -\frac{1}{2} \begin{pmatrix} 4h & 0 & 0 & u \\ 0 & 0 & v & 0 \\ 0 & v & 0 & 0 \\ u & 0 & 0 & -4h \end{pmatrix}. \quad (\text{A1})$$

The eigenvalues are given by

$$\lambda_1 = -\frac{1}{2}v \quad \lambda_3 = -\frac{1}{2}\sqrt{16h^2 + u^2} \quad (\text{A2})$$

$$\lambda_2 = \frac{1}{2}v \quad \lambda_4 = \frac{1}{2}\sqrt{16h^2 + u^2}, \quad (\text{A3})$$

and the corresponding (unnormalized) eigenvectors by

$$\mathbf{u}_1^T = (0, 1, 1, 0) \quad (\text{A4})$$

$$\mathbf{u}_2^T = (0, -1, 1, 0) \quad (\text{A5})$$

$$\mathbf{u}_3^T = \left( \frac{4h + \sqrt{16h^2 + u^2}}{u}, 0, 0, 1 \right) \quad (\text{A6})$$

$$\mathbf{u}_4^T = \left( \frac{4h - \sqrt{16h^2 + u^2}}{u}, 0, 0, 1 \right). \quad (\text{A7})$$

#### 2. N=3

The Hamiltonian for the three-site LMG system is given by

$$H_3 = -\frac{1}{3} \begin{pmatrix} 9h & 0 & 0 & -u & 0 & -u & -u & 0 \\ 0 & 3h & v & 0 & v & 0 & 0 & -u \\ 0 & v & 3h & 0 & v & 0 & 0 & -u \\ -u & 0 & 0 & -3h & 0 & v & v & 0 \\ 0 & v & v & 0 & 3h & 0 & 0 & -u \\ -u & 0 & 0 & v & 0 & -3h & v & 0 \\ -u & 0 & 0 & v & 0 & v & -3h & 0 \\ 0 & -u & -u & 0 & -u & 0 & 0 & -9h \end{pmatrix}, \quad (\text{A8})$$

leading to the eigenvalues

$$\mu_{1,2} = \frac{1}{3}(v - 3h) \quad \mu_{3,4} = \frac{1}{3}(v + 3h) \quad (\text{A9})$$

$$\mu_5 = \frac{1}{3}(-3h - v - \Delta_-) \quad (\text{A10})$$

$$\mu_6 = \frac{1}{3}(-3h - v + \Delta_-) \quad (\text{A11})$$

$$\mu_7 = \frac{1}{3}(3h - v - \Delta_+) \quad (\text{A12})$$

$$\mu_8 = \frac{1}{3}(3h - v + \Delta_+) \quad (\text{A13})$$

and eigenvectors

$$\mathbf{v}_1^T = (0, -1, 0, 0, 1, 0, 0, 0) \quad (\text{A14})$$

$$\mathbf{v}_2^T = (0, -1, 1, 0, 0, 0, 0, 0) \quad (\text{A15})$$

$$\mathbf{v}_3^T = (0, 0, 0, -1, 0, 0, 1, 0) \quad (\text{A16})$$

$$\mathbf{v}_4^T = (0, 0, 0, -1, 0, 1, 0, 0) \quad (\text{A17})$$

$$\mathbf{v}_5^T = \left( \frac{\delta_+ - \Delta_-}{u}, 0, 0, 1, 0, 1, 1, 0 \right) \quad (\text{A18})$$

$$\mathbf{v}_6^T = \left( \frac{\delta_+ + \Delta_-}{u}, 0, 0, 1, 0, 1, 1, 0 \right) \quad (\text{A19})$$

$$\mathbf{v}_7^T = \left( 0, \frac{\delta_- - \Delta_+}{3u}, \frac{\delta_- - \Delta_+}{3u}, 0, \frac{\delta_- - \Delta_+}{3u}, 0, 0, 1 \right) \quad (\text{A20})$$

$$\mathbf{v}_8^T = \left( 0, \frac{\delta_- + \Delta_+}{3u}, \frac{\delta_- + \Delta_+}{3u}, 0, \frac{\delta_- + \Delta_+}{3u}, 0, 0, 1 \right) \quad (\text{A21})$$

where  $\Delta_\pm = 2\sqrt{1 + 9h^2 \pm 3hv + \gamma u}$  and  $\delta_\pm = -6h \pm v$ .

### 3. N=4

The Hamiltonian of a four-site LMG system may be expressed in a block-diagonal form given by

$$H_4 = \begin{pmatrix} A & 0 & \cdots & 0 \\ 0 & B & \cdots & 0 \\ 0 & \cdots & B & 0 \\ 0 & \cdots & 0 & C \end{pmatrix} \quad (\text{A22})$$

where

$$A = -\frac{1}{4} \begin{pmatrix} 16h & 0 & -\sqrt{6}u & 0 & 0 \\ 0 & 3v+8h & 0 & -3u & 0 \\ -\sqrt{6}u & 0 & 4v & 0 & -\sqrt{6}u \\ 0 & -3u & 0 & 3v-8h & 0 \\ 0 & 0 & -\sqrt{6}u & 0 & -16h \end{pmatrix} \quad (\text{A23})$$

$$B = \frac{1}{4} \begin{pmatrix} v-8h & 0 & u \\ 0 & 0 & 0 \\ u & 0 & v+8h \end{pmatrix} \quad (\text{A24})$$

$$C = \frac{1}{4} \begin{pmatrix} 2v & 0 & 0 & 0 & 0 \\ 0 & v-8h & 0 & u & 0 \\ 0 & 0 & 0 & u & 0 \\ 0 & u & 0 & v+8h & 0 \\ 0 & 0 & 0 & 0 & 2v \end{pmatrix}. \quad (\text{A25})$$

- [1] S. Sachdev, *Quantum Phase Transitions* (Cambridge University Press, Cambridge, 1999).
- [2] L. Amico, R. Fazio, A. Osterloh and V. Vedral, *Rev. Mod. Phys.* **80**, 517 (2008).
- [3] P. Zanardi and N. Paunkovic, *Phys. Rev. E* **74**, 031123 (2006).
- [4] P. Zanardi, M. Cozzini and P. Giorda, *J. Stat. Mech.: Theory Exp.* L020022 (2007).
- [5] M. Cozzini, P. Giorda and P. Zanardi, *Phys. Rev. B* **75**, 014439 (2007).
- [6] P. Zanardi, P. Giorda and M. Cozzini, *Phys. Rev. Lett.* **99**, 100603 (2007).
- [7] M. Prokopenko, J. T. Lizier, O. Obst and X. R. Wang *Phys. Rev. E* **84**, 041116 (2011).
- [8] P. Zanardi, M. G. A. Paris, L. Campos-Venuti, *Phys. Rev. A* **78**, 042105 (2008).
- [9] C. Invernizzi, M. Korbmann, L. Campos-Venuti and M. G. A. Paris, *Phys. Rev. A* **78**, 042106 (2008).
- [10] C. Invernizzi and M.G.A. Paris, *J. Mod. Opt.* **57**, 198 (2010).
- [11] C. W. Helstrom, *Quantum Detection and Estimation Theory* (Academic Press, New York, 1976).
- [12] M. G. A. Paris, *Int. J. Quant. Inf.* **7**, 125 (2009).
- [13] L. Campos-Venuti and P. Zanardi *Phys. Rev. Lett.* **99**, 095701 (2007).
- [14] S. Garnerone, N. T. Jacobson, S. Haas, and P. Zanardi, *Phys. Rev. Lett.* **102**, 057205 (2009).
- [15] S. N. Khanna and A. W. Castleman, *Quantum Phenomena in Clusters and Nanostructures* (Springer, Berlin, 2003).
- [16] D. Tsomokos, S. Ashhab and F. Nori, *New J. Phys.* **10** (2008) 113020.
- [17] D. Gatteschi, R. Sessoli, and J. Villain, *Molecular Nanomagnets* (Oxford University Press, Oxford, 2006).
- [18] F. Troiani and P. Zanardi, *Phys. Rev. B* **88**, 094413 (2013).
- [19] H. J. Lipkin, N. Meshkov and A. J. Glick, *Nucl. Phys.* **62**, 188 (1965).
- [20] N. Meshkov, A. J. Glick, and H. J. Lipkin *Nucl. Phys.* **62**, 199 (1965).
- [21] A. J. Glick, H. J. Lipkin and N. Meshkov *Nucl. Phys.* **62**, 211 (1965).
- [22] D. A. Garanin, X. Martinez Hidalgo and E. M. Chudnovsky, *Phys. Rev. B* **57**, 13639 (1998).
- [23] S. Dusuel and J. Vidal *Phys. Rev. Lett.* **93**, 237204 (2004).
- [24] S. Dusuel and J. Vidal *Phys. Rev. B* **71**, 224420 (2005).
- [25] H. Wichterich, J. Vidal and S. Bose, *Phys. Rev. A* **81**, 032311 (2010).
- [26] J. Ma and X. Wang, *Phys. Rev. A* **80**, 012318 (2009).
- [27] H. M. Kwok, W. Q. Ning, S. J. Gu, H. Q. Lin, *Phys. Rev. E* **78**, 032103 (2008).
- [28] J. Ma, X. Wang, and S.-J. Gu, *Phys. Rev. E* **80**, 021124 (2009).
- [29] O. Castaños, R. López-Peña, E. Nahmad-Achar and J. G. Hirsch, *J. Phys.: Conf. Ser.* **387**, 012021 (2012).
- [30] T. Caneva, R. Fazio and G. E. Santoro, *Phys. Rev. B* **78**, 104426 (2008).
- [31] T. Caneva, R. Fazio and G. E. Santoro, *J. Phys. Conf. Ser.* **143**, 012004 (2009).
- [32] P. Solinas, P. Ribeiro, R. Mosseri, *Phys. Rev. A* **78**, 052329 (2008).
- [33] I. Fuentes-Schuller, P. Barberis-Blostein, *J. Phys. A* **40**, F601 (2007).
- [34] A. Micheli, D. Jaksch, J. I. Cirac, and P. Zoller, *Phys. Rev. A* **67**, 013607 (2003).
- [35] S. Morrison and A. S. Parkins *Phys. Rev. Lett.* **100**, 040403 (2008).
- [36] G. Chen, J. Q. Liang and S. Jia, *Opt. Expr.* **17** 19682 (2009).
- [37] J. Larson *EPL* **90** 54001 (2010).
- [38] R. G. Unanyan and M. Fleischhauer, *Phys. Rev. Lett.* **90**, 133601 (2003).
- [39] F. Pan, J. Draayer, *Phys. Lett. B* **451**, 1 (1999).
- [40] G. Rosensteel, D. J. Rowe, S. Y. Ho, *J. Phys. A* **41**, 025208 (2008).
- [41] O. Castaños, R. López-Peña, J. G. Hirsch, and E. López-Moreno, *Phys Rev B* **74**, 104118 (2006).
- [42] P. Ribeiro, J. Vidal, R. Mosseri, *Phys. Rev. Lett.* **99**, 050402 (2007).
- [43] P. Ribeiro, J. Vidal, R. Mosseri, *Phys. Rev. E* **78**, 021106 (2008).
- [44] R. Botet, R. Jullien, and P. Pfeuty, *Phys. Rev. Lett.* **49**, 478 (1982).
- [45] R. Botet and R. Jullien, *Phys. Rev. B* **28**, 3955 (1983).
- [46] V. V. Ulyanov, O. B. Zaslavskii, *Phys. Rep.* **216**, 179 (1992).
- [47] M. Brunelli, S. Olivares, M. G. A. Paris, *Phys. Rev. A* **84**, 032105 (2011).
- [48] M. Brunelli, S. Olivares, M. Paternostro, M. G. A. Paris, *Phys. Rev. A* **86**, 012125 (2012).